ACS Pharmacology & Translational Science

pubs.acs.org/ptsci

Article

Targeting Functional Activity of AKT Has Efficacy against Aggressive Neuroblastoma

Marion Le Grand, Kathleen Kimpton, Christine C. Gana, Emanuele Valli, Jamie I. Fletcher, and Maria Kavallaris*

Cite This: *ACS Pharmacol. Transl. Sci.* 2020, 3, 148–160

Read Online

ACCESS | Metrics & More | Article Recommendations | Supporting Information

ABSTRACT: *MYCN*-amplified neuroblastoma is one of the deadliest forms of childhood cancer and remains a significant clinical challenge. Direct pharmacological inhibition of MYCN is not currently achievable. One strategy could be to target the AKT/GSK3β pathway, which directly regulates the stability of the MYCN protein. Numerous potent and isoform-specific small-molecule AKT inhibitors have been developed. However, the selection of the right drug combinations in the relevant indication will have a significant impact on AKT inhibitor clinical success. To maximally exploit the potential of AKT inhibitors, a better understanding of AKT isoform functions in cancer is crucial. Here using RNAi to downregulate specific AKT isoforms, we demonstrated that loss of total AKT activity rather than isoform-specific expression was necessary to decrease MYCN expression and cause a significant decrease in neuroblastoma cell proliferation. Consistent with these observations, isoform-specific pharmacological inhibition of AKT was substantially less effective than pan-AKT inhibition in combination with cytotoxic drugs in *MYCN*-amplified neuroblastoma. The allosteric pan-AKT inhibitor perifosine had promising *in vitro* and *in vivo* activity in combination with conventional cytotoxic drugs in *MYCN*-amplified neuroblastoma cells. Our results demonstrated that perifosine drug combination was able to induce apoptosis and downregulate ABC transporter expression. Collectively, this study shows that selecting pan-AKT inhibitors rather than isoform-specific drugs to synergize with first-line chemotherapy treatment should be considered for clinical trials for aggressive neuroblastoma and, potentially, other MYCN -driven cancers.

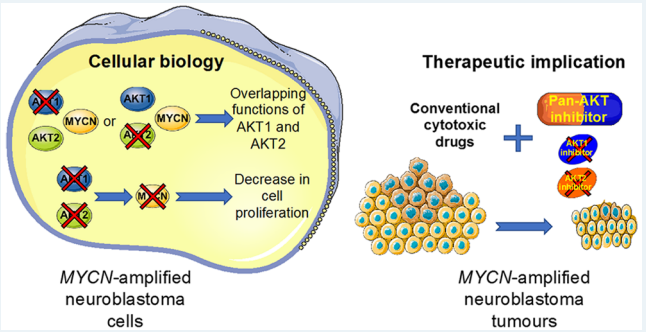

KEYWORDS: *AKT, MYCN, neuroblastoma, pan-AKT inhibitor*

Neuroblastoma is an enigmatic, multifaceted tumor of the peripheral nervous system that represents the most common solid tumor in children under 5.[1] On the basis of its cellular and biological heterogeneity, neuroblastoma behavior can range from low-risk cancers with a tendency toward spontaneous regression to high-risk ones with extensive growth, early metastasis, and a poor prognosis.[2,3] Members of the Myc family of transcription factors (c-Myc, MYCN, and L-Myc) play critical roles in many cellular processes required for tumorigenesis including cell growth and differentiation, metabolism, and genome stability.[4] Amplification of the *MYCN* oncogene is observed in approximately 25% of neuroblastoma patients and is a validated initiator of tumorigenesis.[5−7] *MYCN* amplification is strongly associated with disease progression, and its amplification status is a key genetic biomarker for risk stratification.[3] The prominent role of *MYCN* in neuroblastoma oncogenesis and the fact that MYCN expression is restricted to tumor tissues postdevelopment imply that MYCN is likely to be an important therapeutic target, presenting a unique opportunity for a targeted strategy in neuroblastoma.[8] Ne-Nevertheless, to date, no effective treatment demonstrating convincing evidence of MYCN inhibition has yet been translated into the clinic. Therapeutic strategies to indirectly target MYCN have emerged, including blocking MYCN-dependent transcription or targeting regulators of *MYCN* mRNA and protein stability.[9]

AKT serine/threonine protein kinases constitute fundamental intracellular signaling systems for the regulation of an ample assortment of cellular and physiological activities, such as cell growth, proliferation and metabolism.[10] The AKT protein kinase family is present in three isoforms: AKT1, AKT2 and AKT3 encoded on three distinct chromosomes and sharing a considerable homology.[11] There is increasing evidence from clinical and laboratory studies that the PI3K/AKT pathway plays an important role in the development and progression of neuroblastoma.[12] AKT drives oncogenic regulation of MYCN

Received: October 18, 2019
Published: January 23, 2020

https://dx.doi.org/10.1021/acsptsci.9b00085
ACS Pharmacol. Transl. Sci. 2020, 3, 148–160

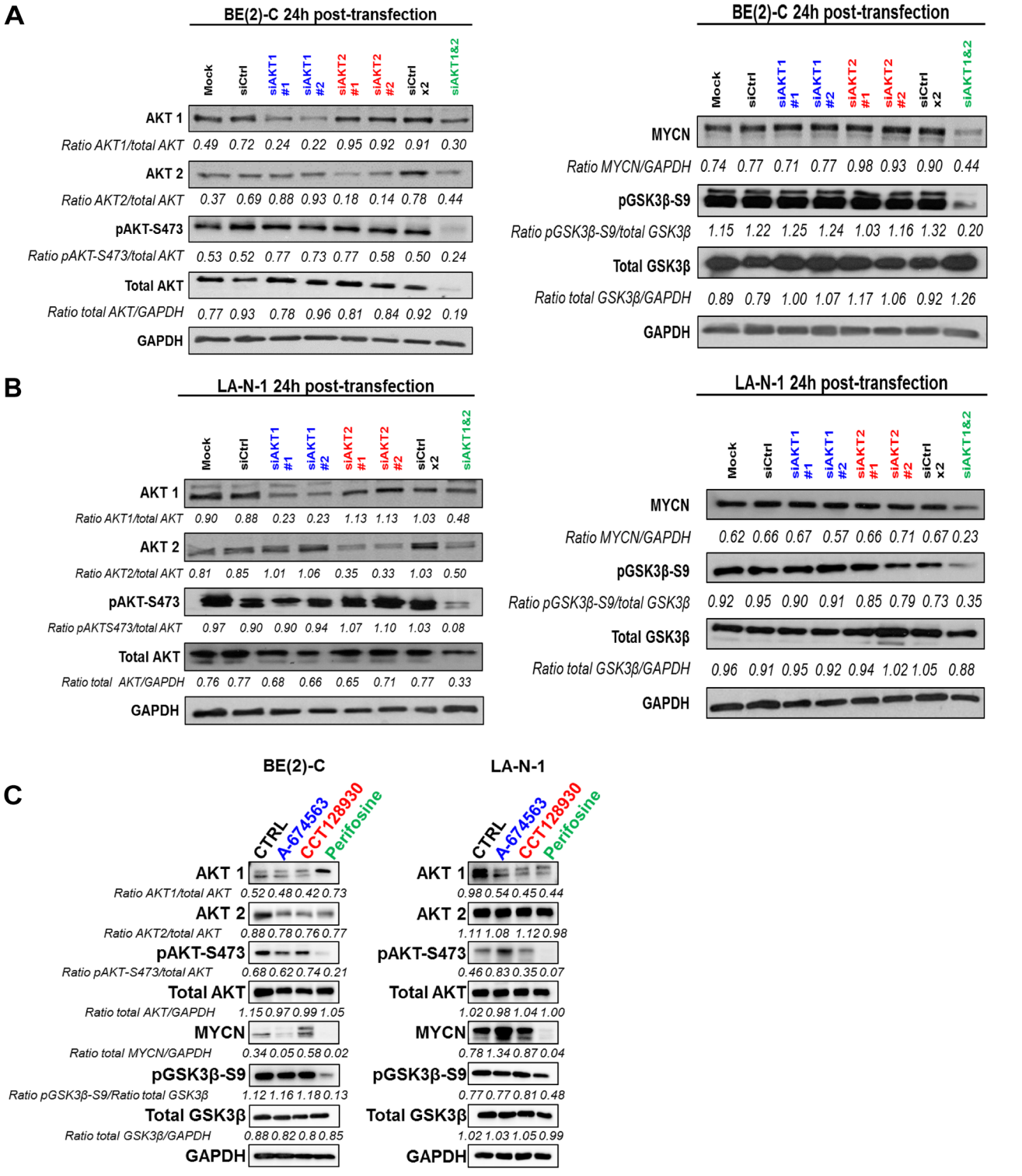

Figure 1. Inhibition of total AKT activity suppresses MYCN expression. (A, B) Western blot analysis of AKT1 or/and AKT2 silencing in protein extracts from (A) BE(2)-C and (B) LA-N-1 cells. Cell lysates were harvested from cells 24 h after transfection with mock, siCtrl, siAKT1, or/and AKT2. Blots were probed with the indicated antibodies. GAPDH was used as a loading control. Ratios are the average of 3 independent analysis. (C) Western blot analysis of 24 h treatment of the IC_{50} concentration of AKT1 inhibitor (A-674563; IC_{50} = 0.4 and 0.25 μM in BE(2)-C and LA-N-1, respectively), AKT2 inhibitor (CCT128930; IC_{50} = 7 and 5 μM in BE(2)-C and LA-N-1, respectively) or pan-AKT inhibitor (perifosine; IC_{50} = 7.5 and 10 μM in BE(2)-C and LA-N-1, respectively) in protein extracts from BE(2)-C and LA-N-1 cells. Blots were probed with the indicated antibodies. GAPDH was used as a loading control. Ratios are the average of 2 independent analysis.

through GSK3β providing a therapeutic rationale to inhibit this pathway in *MYCN*-amplified neuroblastoma.[13,14] Preclinical and clinical trials testing AKT inhibitors are ongoing to assess whether their potential will translate to clinical efficacy.[15,16] Improved understanding of the specific functions attributed to the three AKT isoforms in cancer has actively contributed to

https://dx.doi.org/10.1021/acsptsci.9b00085
ACS Pharmacol. Transl. Sci. 2020, 3, 148−160

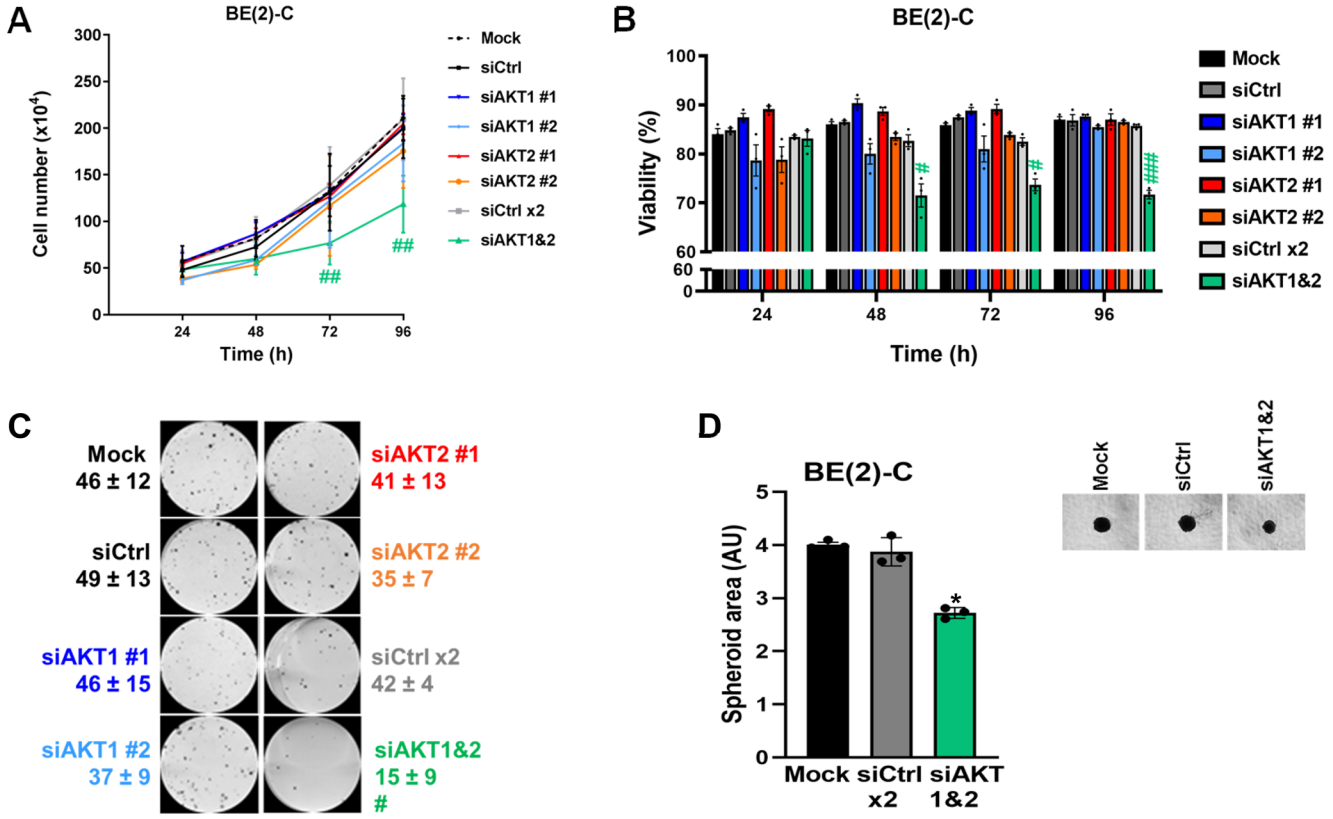

Figure 2. Functional inhibition of total AKT activity is associated with a decrease in neuroblastoma cell proliferation. (A) Cell number and (B) cell viability analysis were performed using Trypan Blue dye exclusion assay on BE(2)-C cells after transfection with mock, control siRNA (siCtrl), and AKT isoform siRNA (siAKT1 nos. 1 and 2, siAKT2 nos. 1 and 2) at the indicated time points. Data are reported as averages (n = 3, ± S.E.M). Statistics were calculated by comparing control siRNA-treated cells with AKT isoform siRNA (#, $p < 0.05$; ##, $p < 0.01$; ###, $p < 0.001$). (C) Representative pictures of clonogenic assay for mock, control siRNA, and AKT isoform-specific siRNA (siAKT1 nos. 1 and 2, siAKT2 nos. 1 and 2). Means of at least three individual assays. Statistics were calculated by comparing the colony number of the control siRNA-treated cells with the AKT isoform-transfected cells. (#, $p < 0.05$). (D) Representative pictures of 3D BE(2)-C spheroids after transfection with mock, siCtrl, siAKT1, and AKT2. Spheroid area (arbitrary unit, AU) was determined at 8 days after cell seeding. Data are reported as averages (n = 3, ± S.E.M). Statistics were calculated by comparing control siRNA-treated cells with AKT isoform siRNA (*, $p < 0.05$).

developing ATP-competitive or allosteric AKT inhibitors targeting specific isoform of AKT or total AKT protein.[17] Indeed, in different solid tumors such as breast, prostate, or lung cancers, AKT isoform-specific or -selective substrate phosphorylation has been demonstrated.[18−20] Moreover, mutations or amplification in *AKT1*−*3* have been reported in different adult cancers such as lung, breast, and endometrial cancers or melanoma.[21−23] In neuroblastoma, no molecular alteration of the AKT isoforms has yet been reported. Opel et al. showed that activation of AKT correlates with poor prognosis in primary neuroblastoma.[24] However, it remains unclear whether AKT isoforms have overlapping or divergent functions in neuroblastoma. Optimal strategies for the clinical development of AKT inhibitors are currently unknown and improving their effectiveness may require a better understanding of AKT isoform functions.

In this study, we addressed the question of how AKT isoforms can play a pivotal role in *MYCN*-amplified neuroblastoma and which small-molecule AKT inhibitors can be promising anticancer compounds in children diagnosed with this cancer. We demonstrate overlapping functions for AKT isoforms in *MYCN*-amplified neuroblastoma, providing a biological rationale for pan-AKT inhibitors in neuroblastoma therapy. We show that the allosteric pan-AKT inhibitor perifosine acts as a drug sensitizer of standard-of-care chemotherapy for patients with *MYCN*-amplified neuroblastoma. Our study therefore allows us to gain insights into the AKT isoform roles in neuroblastoma revealing the interest of pan-AKT inhibitors rather than isoform-specific AKT drugs to develop new anticancer strategies in neuroblastoma.

RESULTS

Activation of AKT Maintains MYCN Expression by Inhibiting GSK3β in Neuroblastoma Cells. Because AKT-mediated GSK3β inhibition is known to drive oncogenic regulation of MYCN,[13,14] we sought to investigate whether specific AKT isoforms may alter MYCN expression in 2 different *MYCN*-amplified neuroblastoma cell lines, BE(2)-C and LA-N-1. In this study, we focused on the isoforms 1 and 2 given that AKT3 protein expression was not detectable in most of the neuroblastoma cell lines tested (Figure S1A). siRNA targeting a specific AKT isoform led, as expected, to a selective decrease in the isoform targeted (Figure 1A,B). In terms of compensatory expression, it appeared that downregulation of AKT1 or AKT2 led to slightly elevated levels of AKT2 or AKT1 expression respectively in both cell lines tested (Figure 1A,B). Knockdown of individual isoforms did not significantly impact AKT phosphorylation level or alter the downstream levels of GSK3β phosphorylation and MYCN expression in either cell line (Figure 1A,B). Nevertheless, simultaneous

https://dx.doi.org/10.1021/acsptsci.9b00085
ACS Pharmacol. Transl. Sci. 2020, 3, 148−160

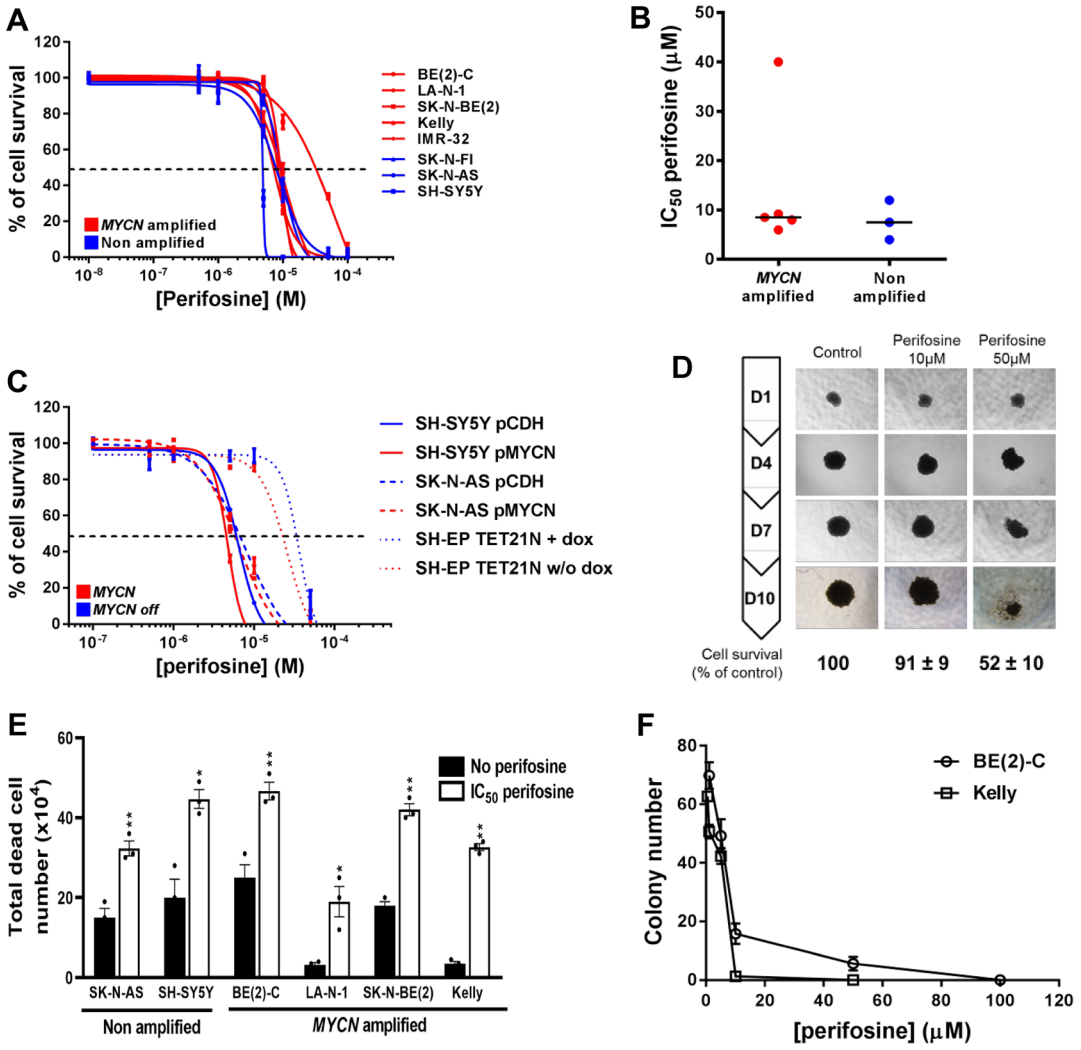

Figure 3. Pan-AKT inhibitor perifosine decreases cell proliferation in 2D and 3D culture neuroblastoma models. (A) Growth inhibition assay performed on a panel of neuroblastoma cell lines using Alamar Blue after 72 h incubation with a range of concentrations of perifosine. Means of at least three individual experiments: bars, SEM; log scale for *x* axis. (B) Plots for the IC_{50} values of perifosine on a panel of neuroblastoma cell lines harboring (n = 5) or lacking (n = 3) *MYCN* amplification. (C) Growth inhibition assay performed in three neuroblastoma cells with *MYCN* expression modulation using Alamar Blue after 72 h incubation with a range of concentrations of perifosine. Means of at least three individual experiments: bars, SEM; log scale for *x* axis. (D) Representative pictures of 3D BE(2)-C spheroids treated with a range of perifosine concentrations. Results were expressed as a percentage of growth in non-treated spheroids at day 10. Mean ± SEM of three independent experiments are shown. (E) Total dead cell number on a panel of neuroblastoma cell lines treated with 72h of the IC_{50} perifosine concentration. Data are reported as averages (n = 3, ± SEM). Statistics were calculated by comparing the untreated cells with perifosine-treated cells (*, $p < 0.05$; **, $p < 0.01$). (F) Clonogenic assays were done on two *MYCN*-amplified neuroblastoma cell lines treated with a range of perifosine concentration. Means of three individual assays; bars, SEM. Statistics were calculated by comparing the colony number of the untreated cells with perifosine-treated cells at each concentration (***, $p < 0.001$).

knockdown of AKT1 and AKT2 expression reduced both phosphorylated AKT and total AKT expression in both cell lines. Loss of AKT was associated with a reduced level of GSK3β phosphorylation without altering total GSK3β level and a substantial decrease in MYCN protein expression (Figure 1A,B). To assess whether these results could have clinical implication for targeting MYCN expression using small-molecule AKT inhibitors, three different commercially available compounds were used: the selective AKT1 inhibitor A-674563, the selective AKT2 inhibitor CCT128930, and the allosteric pan-AKT inhibitor perifosine. In agreement with results obtained with gene silencing, the pan-AKT inhibitor perifosine was substantially more effective at reducing MYCN protein expression in BE(2)-C and LA-N-1 cell lines through an inhibition of AKT phosphorylation and activation of GSK3β (Figure 1C). Collectively, these results demonstrate that MYCN expression is regulated by total AKT activity rather than specific AKT isoform in *MYCN*-amplified neuroblastoma cells.

Functional or Pharmacological Inhibition of total AKT Activity Leads to a Decrease in Neuroblastoma Cell Proliferation. To determine whether the activity of individual AKT isoforms impacts on cell proliferation and viability, BE(2)-C and LA-N-1 cells were assessed in short- and long-term assays following knockdown of AKT1, AKT2, or both isoforms. Downregulation of individual isoforms did not significantly alter cell proliferation (Figures 2A and S1B) or viability (Figures 2B and S1C) in either short-term assay or long-term colony formation assay (Figure 2C). In contrast, dual AKT1−AKT2 knockdown significantly reduced BE(2)-C

https://dx.doi.org/10.1021/acsptsci.9b00085
ACS Pharmacol. Transl. Sci. 2020, 3, 148−160

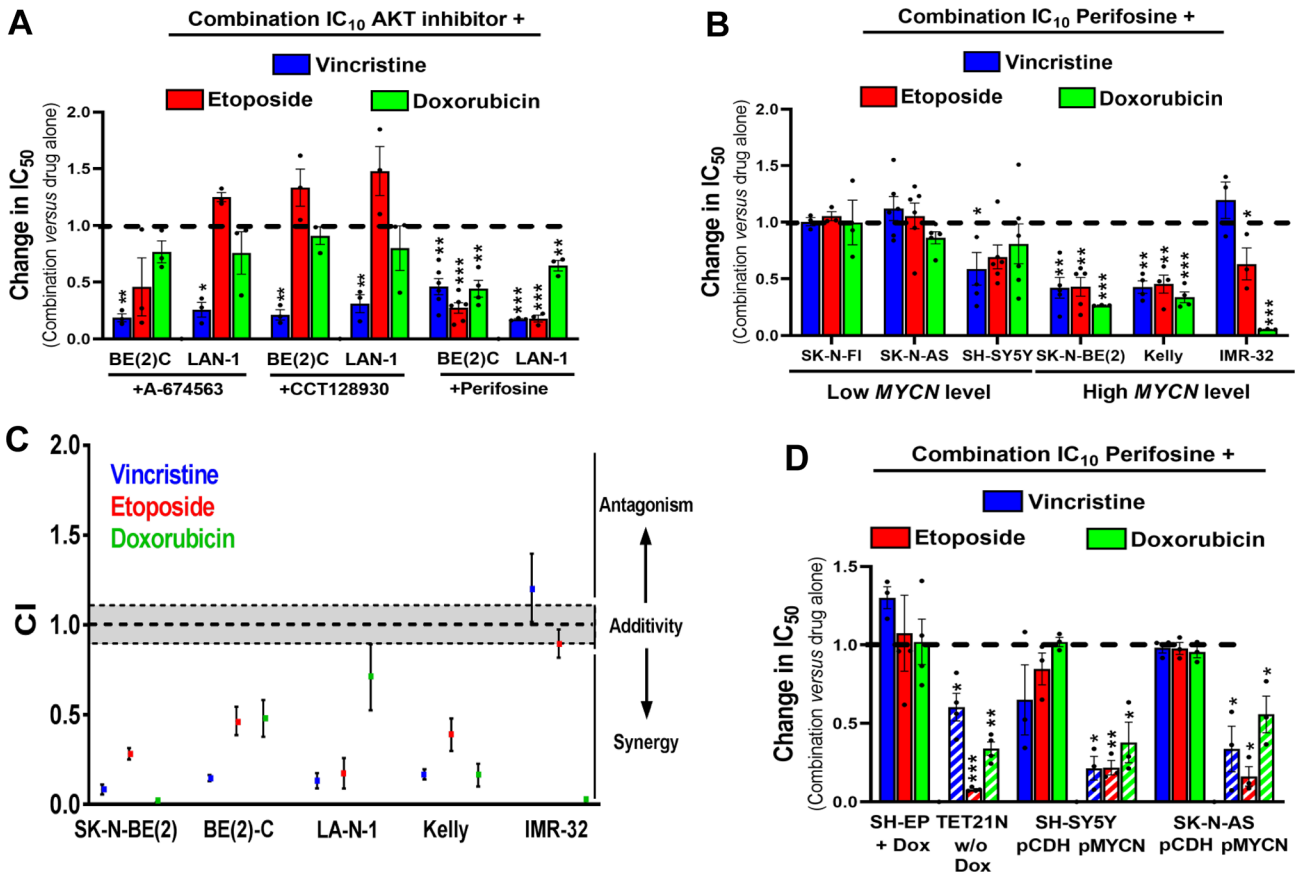

Figure 4. High *MYCN* expression sensitizes neuroblastoma cells to the combination of pan-AKT inhibitor with conventional cytotoxic drugs. (A) Histogram representation of change in IC_{50} values in two different neuroblastoma cell lines when chemotherapy agents are used in combination with subtoxic concentrations of AKT inhibitors (IC_{10}) A-674563, CCT128930, or perifosine. (B) Histogram representation of change in IC_{50} values in a panel of neuroblastoma cells when chemotherapy agents are used in combination with subtoxic concentrations of perifosine (IC_{10}). (C) Dot plot representation of the combination indexes (CI) of chemotherapeutic agents combined to IC_{10} perifosine in *MYCN*-amplified neuroblastoma cells. (D) Histogram representation of change in IC_{50} values in three neuroblastoma cells with *MYCN* expression modulation when chemotherapy agents are used in combination with subtoxic concentrations of perifosine (IC_{10}). Columns are the means of at least four individual experiments; bars are the SEM. Statistical analysis was performed by comparing the IC_{50} values of chemotherapy alone or in combination with perifosine using Student's *t*-test (*, $p < 0.05$; **, $p < 0.01$; ***, $p < 0.001$).

cell proliferation by 43 ± 7% ($p < 0.01$, Figure 2A) and cell viability by 18 ± 6% ($p < 0.001$, Figure 2B) at 96 h post-transfection in comparison to siRNA control and the colony number was reduced from 42 ± 4 in control cells to 15 ± 9 colonies ($p < 0.05$, Figure 2C). Comparable results were obtained in the LA-N-1 cell line (Figure S1B,C). The impact of AKT1−AKT2 knockdown on cell growth was maintained in a BE(2)-C 3D-tumor spheroid culture where the spheroid area was reduced from 3.8 ± 0.3 in control cells to 2.6 ± 0.1 ($p < 0.05$, Figure 2D). Together, these results indicate that isoform-specific AKT inhibition is unlikely to be as effective as pan-AKT inhibition for treating neuroblastoma and provides a rationale to move on to the use of the pan-AKT inhibitor perifosine.

A panel of eight high-risk neuroblastoma cell lines, five with *MYCN* amplification and three without (Figure S2A), was assessed for sensitivity to the pan-AKT inhibitor perifosine in dose−response assays. Perifosine significantly reduced cell survival with IC_{50} values ranging from 4 ± 0.3 to 55 ± 3 μM, that are achievable *in vivo* (Figure 3A). Overall, mean IC_{50} values were not significantly different between *MYCN*-amplified and non-amplified neuroblastoma cell lines (14.3 ± 6.4 *vs* 8.7 ± 2.3 μM, respectively; $p = 0.3857$; Figure 3B). Our result is supported by mining the publically available GDSC (Genomics of Drug Sensitivity in Cancer) database, which integrates anticancer drug responses on cancer cell lines (www.cancerRxgene.org). Analysis of 2 different pan-AKT inhibitors (AKT inhibitor VIII and MK-2206) in a panel of 24 neuroblastoma cell lines (18 with *MYCN*-amplification and 6 without *MYCN* amplification) showed no significant drug sensitivity depending on *MYCN* status (Figure S2B). Moreover, the same results have been observed with both selective-isoform AKT inhibitors in 6 different neuroblastoma cell lines (Figure S2C,D). To further investigate any potential relationship between perifosine sensitivity and *MYCN* amplification status, we utilized the SH-EP/Tet21N human neuroblastoma cell line, in which exogenous MYCN expression can be repressed by doxycycline (Figure S2E), and two non-*MYCN*-amplified neuroblastoma cell lines, SH-SY5Y and SK-N-AS, stably overexpressing MYCN (Figure S2F). For each cell line, expression of MYCN did not significantly alter the perifosine IC_{50} values (Figure 3C, $p = 0.8324$, 0.9381, and 0.9042 respectively for SH-SY5Y, SK-N-AS, and SH-EP/Tet21N). The dose-dependent cytotoxic effect of perifosine was confirmed in a BE(2)-C 3D-tumor spheroid neuroblastoma cell model (Figure 3D). We further observed that perifosine

https://dx.doi.org/10.1021/acsptsci.9b00085
ACS Pharmacol. Transl. Sci. 2020, 3, 148−160

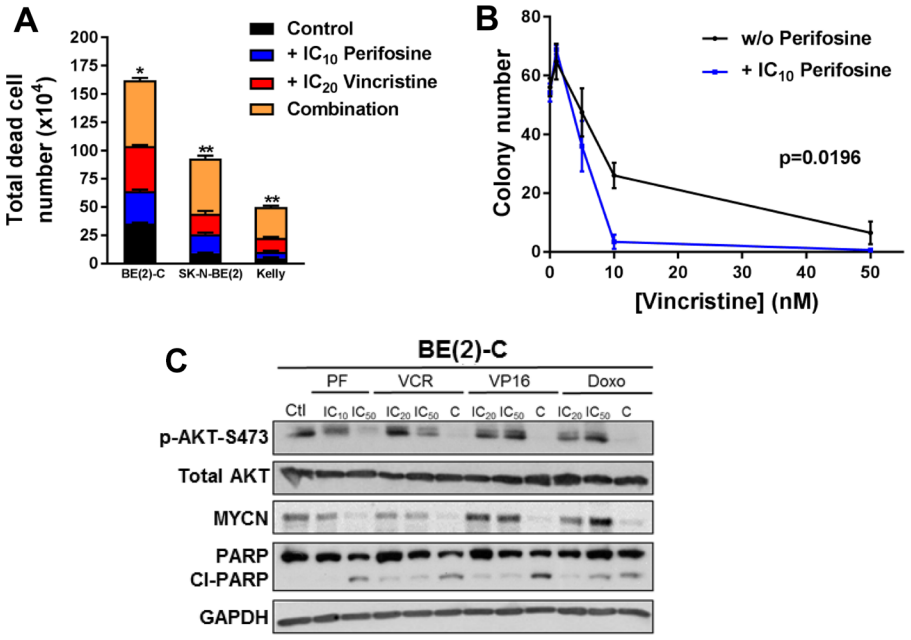

Figure 5. Low doses of perifosine enhance the cytotoxic drug activities in *MYCN*-amplified BE(2)-C cells. (A) Total dead cell number performed using Trypan Blue dye exclusion assay on a panel of three *MYCN*-amplification neuroblastoma cell lines treated for 72 h of the IC_{10} perifosine concentration alone, IC_{20} vincristine alone, or their combination. Data are reported as averages (n = 3, ± SEM). Statistics were calculated by comparing the cytotoxic agent-treated cells with the combination-treated cells (*, $p < 0.05$; **, $p < 0.01$). (B) Clonogenic assays were done on BE(2)-C cells treated with a range of vincristine alone (black line) or combined with IC10 perifosine (blue line). Data are reported as averages (n = 3, ± SEM). Extra sum of F^2 test was used to determine statistical significance between nonlinear regression of vincristine alone versus combination treatment. (C) Western blot analysis in protein extracts from BE(2)-C cells after 48 h of treatment of IC_{10} or IC_{50} of perifosine alone (PF), IC_{20} or IC_{50} of cytotoxic drug alone (VCR: vincristine, VP16: etoposide and Doxo: doxorubicin), or their combination (C: combination of IC_{10} perifosine with IC_{20} cytotoxic drug). Blots were probed with the indicated antibodies. GAPDH was used as a loading control.

led to a marked decrease in cell viability by increasing the total dead cell number (Figure 3E) as well as a decrease in the colony number (Figure 3F) in a panel of neuroblastoma cells.

Pan-AKT Inhibitor Perifosine Potentiates the *in Vitro* Activity of Chemotherapy Drugs Selectively in *MYCN*-Amplified Neuroblastoma. Because monotherapies are unlikely to cure cancer, in order to identify potential synergistic drug interactions, we next tested isoform-selective or pan-AKT inhibitors in combination with three standard-of-care chemotherapy agents used to treat high-risk neuroblastoma: the microtubule-targeting agent vincristine, the topoisomerase II inhibitor etoposide, and the anthracycline agent doxorubicin. A minimally cytotoxic concentration of each AKT inhibitor (IC_{10}) was combined with a range of concentrations of each cytotoxic agent. The AKT1 inhibitor A-674563, the AKT2 inhibitor CCT128930, and the pan-AKT inhibitor perifosine all sensitized BE(2)-C and LA-N-1 cells to vincristine; however, sensitization to etoposide or doxorubicin was only observed with perifosine (Figure 4A). The same trend was confirmed with the AKT1/2 allosteric inhibitor MK-2206 (Figure S3A). Expansion of perifosine data to a panel of 6 neuroblastoma cell lines suggests that pan-AKT inhibition is more efficient to potentiate chemotherapy in *MYCN*-amplified neuroblastoma cell lines (Figure 4B). Combination index (CI) calculations indicate synergistic interactions for most of the combinations tested (CI < 1; Figure 4C). These results were confirmed in BE(2)-C cells grown in 3D-tumor spheroid culture, where perifosine sensitized cells to both vincristine and doxorubicin (Figure S3B). As synergy between AKT inhibitors and conventional chemotherapy was only observed in *MYCN*-amplified cell lines, we assessed synergy in *MYCN*-inducible SH-EP/Tet21N cells and SH-SY5Y and SK-N-AS cells stably overexpressing MYCN (Figure S2E,F). Perifosine sensitized all three cell lines to vincristine, etoposide, and doxorubicin when MYCN was overexpressed, but not in the absence of exogenous MYCN expression (Figure 4D).

All combinations tested in three *MYCN*-amplified neuroblastoma cell lines led to a decrease in cell viability as reflected by a significant increase in total dead cells (Figures 5A and S3C). Moreover, IC_{10} of perifosine (2.5 μM) combined with a range of vincristine or doxorubicin concentrations significantly decreased colony formation (p = 0.0196 and 0.0029, respectively, Figures 5B and S3D), which is not the case combined with etoposide (p = 0.3033). To confirm that the efficacy seen with perifosine and cytotoxic drugs in combination was associated with inhibition of AKT activity, AKT phosphorylation was analyzed as a biomarker. After 48 h, treatment with IC_{50} of perifosine (7.5 μM) or vincristine (45 nM), but not with etoposide (10 μM) or doxorubicin (200 nM), led to a decrease in the phosphorylated active form of AKT in a dose-dependent manner (Figure 5C). In all tested cotreatments combining the two lowest drug concentrations (IC_{10} of perifosine with IC_{20} of cytotoxic drugs), we observed a strong inhibition of the AKT phosphorylation associated with downregulation of MYCN expression. Moreover, perifosine combination therapy led to an increase of cleaved PARP, an apoptotic marker (Figure 5C). The ABC transporters P-gp and MRP1 confer resistance to vincristine[25] and may be mechanisms limiting its efficacy in childhood cancer.[26] We therefore tested the effect of AKT inhibition on P-gp and MRP1 expression, using BE(2)-C cells, which express high levels of both transporters. Perifosine treatment at its IC_{50} (7.5

https://dx.doi.org/10.1021/acsptsci.9b00085
ACS Pharmacol. Transl. Sci. 2020, 3, 148−160

Table 1. Median Survival of Nude Mice Harboring *MYCN*-Amplified BE(2)-C or Non-amplified SK-N-AS Xenograft Tumors

	treatment (mice per cohort)	median survival (days)	log-rank test (vs vehicle)	log-rank test (vs perifosine)	log-rank test (vs vincristine)
xenograft model of BE(2)-C	vehicle (n = 8)	18	N/A	0.132	0.541
	perifosine (n = 8) 20 mg/kg per os, 5 days per week	20	0.132	N/A	0.529
	vincristine (n = 8) 0.2 mg/kg i.v., 5 days	20	0.541	0.529	N/A
	vincristine + perisofine (n = 7)	31	**0.016**	**0.039**	**0.026**
xenograft model of SK-N-AS	vehicle (n = 8)	21	N/A	0.33	0.369
	perifosine (n = 8) 15 mg/kg per os, 5 days per week	19	0.33	N/A	0.455
	vincristine (n = 8) 0.2 mg/kg i.v., 5 days	26	0.369	0.455	N/A
	vincristine + perisofine (n = 8)	28	**0.008**	**0.003**	0.063

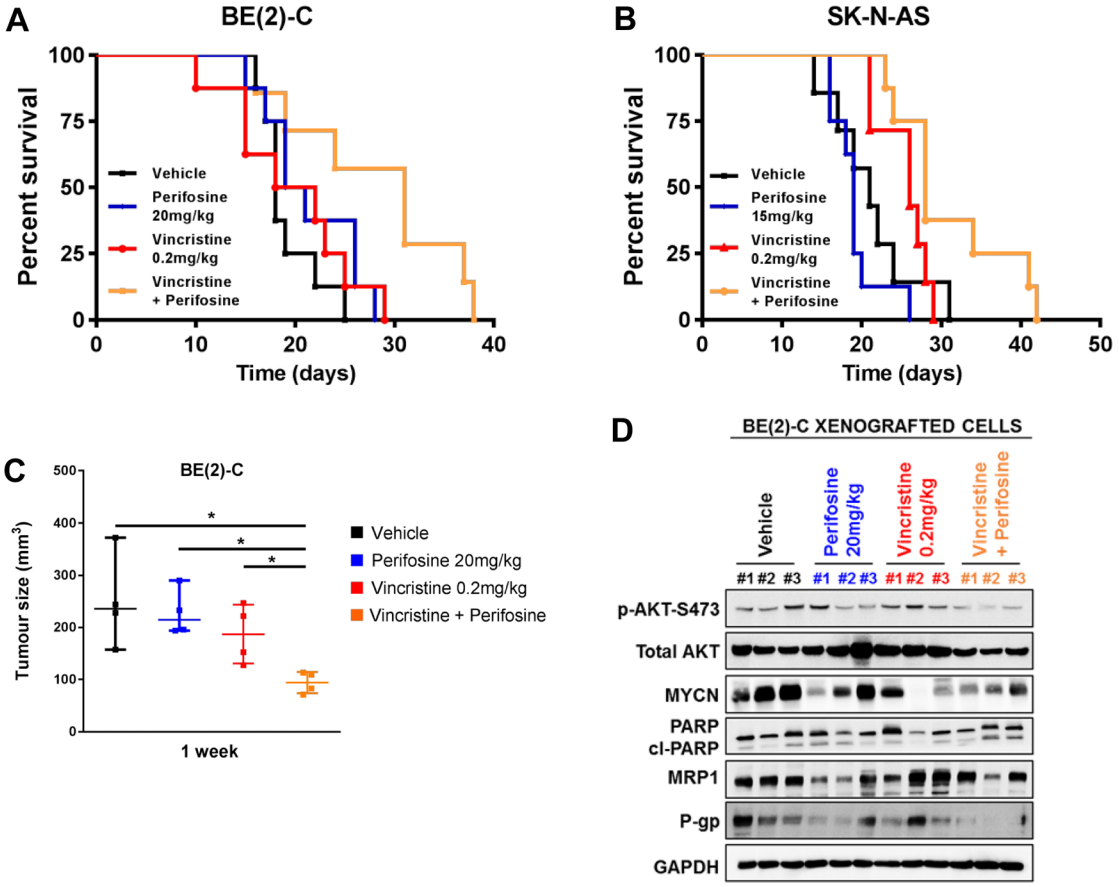

Figure 6. Perifosine synergizes with vincristine in a *MYCN*-amplified xenografted neuroblastoma model. (A, B) Perifosine was administered by oral gavage 5 days/week throughout the study, and vincristine was administered by i.v. once daily for the first 5 days. Kaplan−Meier survival curves (n = 8/group) of BE(2)-C (A) or SK-N-AS (B) tumor-grafted mice treated by vehicle (black), perifosine alone (blue), vincristine alone (red), or their combination (orange). (C) Tumors were collected after 1 week of treatment, and tumor size was determined in the different groups in nude mice harboring *MYCN*-amplified BE(2)-C xenograft tumors (n = 4/group; Student's t-test; *, $p < 0.05$). (D) Western blot analysis in protein extracts from BE(2)-C xenografted cells after 1 week of treatment of vehicle (black), perifosine 20 mg/kg (oral gavage, daily, blue), vincristine 0.2 mg/kg (i.v. 5 days, red), and the combination vincristine with perifosine (orange). n = 3 different mice/group. Blots were probed with the indicated antibodies. GAPDH was used as a loading control.

μM) decreased MRP1 expression *in vitro*, while dual AKT1−AKT2 knockdown by siRNA reduced both MRP1 and P-gp expression (Figure S4A). To determine whether ABC transporter inhibition increased the efficacy of the perifosine/vincristine combination, we used the dual MRP1 and P-gp inhibitor reversan.[27] As expected, 5 μM reversan (IC_{10}) strongly sensitized cells to vincristine (Figure S4B). However, only a small trend was observed to increase the perifosine/vincristine combination when combined with reversan (Figure S4B). Finally, in all tested cotreatments combining the two lowest drug concentrations (IC_{10} of perifosine with IC_{20} of cytotoxic drugs), we observed a decrease in P-gp expression, whereas only a small trend to decrease in MRP1 is observed (Figure S4C).

Perifosine Potentiates *in Vivo* the Antitumor Efficacy of Vincristine against *MYCN*-Amplified Neuroblastoma. To determine whether the combination of low dose perifosine and vincristine is effective *in vivo*, and whether the combination requires *MYCN* amplification to be efficacious, we utilized two cell line xenograft models of high-risk neuroblastoma, the

https://dx.doi.org/10.1021/acsptsci.9b00085
ACS Pharmacol. Transl. Sci. 2020, 3, 148−160

MYCN-amplified BE(2)-C cell line and non-amplified cell line SK-N-AS. We first performed a pilot study to access the dose response of perifosine and vincristine as single agents (Figure S5A−D). For the drug combination study, we used a subtoxic dose of perifosine (20 mg/kg or 15 mg/kg daily oral respectively for BE(2)-C and SK-N-AS) with a cytotoxic concentration of vincristine (0.2 mg/kg intravenously (i.v.) for 5 days). For both xenograft models, neither perifosine or vincristine alone extended median survival significantly beyond the 18 and 21 days observed for the vehicle control mice for BE(2)-C and SK-N-AS, respectively ($p > 0.1$ for each, Table 1 and Figures 6A,B). The combination of perifosine and vincristine significantly increased median survival to 31 days and 28 days in comparison to the vehicle control mice and the perifosine treated mice ($p = 0.016$ and 0.039 *vs* vehicle and perifosine and $p = 0.008$ and 0.003 *vs* vehicle and perifosine for BE(2)-C and SK-N-AS xenograft models, respectively, Table 1 and Figures 6A,B). However, only the combination of vincristine and perifosine in BE(2)-C xenograft models resulted in a significant median survival increase in comparison to the vincristine control mice ($p = 0.026$, Table 1 and Figure 6A). The schedules used were well-tolerated and did not result in significant change in animal weight in either xenograft model (Figure S5E,F). Next, we carried out a short-term *in vivo* study for the *MYCN*-amplified BE(2)-C xenografts. Measurement of tumor size at 1 week post-treatment yielded a volume from 250 ± 45 mm^3 in control cells to 228 ± 22, 187 ± 28, and 94 ± 10 mm^3, respectively, in mice treated with perifosine, vincristine, and the combination of both drugs ($p < 0.05$, Figure 6C). Finally, immunoblot analysis on tumor samples revealed an increase in cleaved-PARP at 1 week post-combination treatment, indicating an increased in cell death (Figure 6D). A trend to lower expression of both MRP1 and P-gp was observed in xenografts treated with perifosine compared to vehicle-tumor samples (Figure 6D). The perifosine/vincristine combination led to a decrease in P-gp expression in comparison to vehicle-treated tumor samples, and no effect was observed in MRP1 expression (Figure 6D). Perifosine/vincristine combination led also to a decrease in AKT activity and MYCN expression in comparison to vehicle-treated tumor samples (Figure 6D).

DISCUSSION

Over the past decade, there have been many advances in our knowledge of the different AKT isoform functions and substrates in cancer.[17] These discoveries associated with the recent gains in structure-based drug discovery have led to the identification of multiple AKT inhibitors, which are currently in clinical development.[16] However, the selection of the right combination partners in the right indication will have a significant impact on AKT inhibitor clinical success. Our results demonstrate that AKT isoforms have overlapping functions in *MYCN*-amplified neuroblastoma. By increasing our knowledge of AKT isoform functions in neuroblastoma, our data provide a preclinical base for the use of pan-AKT inhibitor rather than AKT-isoform specific compounds as a drug sensitizer in patients with *MYCN*-amplified neuroblastoma.

We still have a limited knowledge about the cellular and molecular mechanisms that determine AKT isoform functional specificity in neuroblastoma. By mining publicly available data and reviewing the literature, we did not find any documented molecular alteration of the AKT isoforms in neuroblastoma. In contrast, in different adult cancers such as lung, breast, and endometrial cancers or melanoma mutations in *AKT1*−*3* have been discovered.[21−23] While AKT mutations predicting AKT inhibitor sensitivity remains to be tested in the clinic, upregulation of AKT3 has already been reported to confer resistance in small-molecule pan-AKT inhibitor MK-2206 in breast cancer.[28] In this study, we were not able to detect AKT3 protein expression in a panel of neuroblastoma cell lines tested, and our results demonstrated that AKT1 and 2 isoforms did not regulate neuroblastoma cell proliferation in a specific manner by contrast with previous data reporting distinct roles of AKT isoforms in regulating breast, lung, or prostate cancer cell proliferation, migration, or survival.[18−20,29] One possible explanation could be AKT isoform compensation. Indeed, the *AKT* genes seem to compensate functionally for one another *in vivo*, as no developmental deficiencies have been observed in any mice lacking only one isoform of the AKT family.[30] It is well-known that the remaining AKT isoforms can compensate for the isoform loss by phosphorylating its substrates. Moreover, a direct regulatory mechanism of AKT gene expression is also possible and has been observed in previous studies.[31−33] In our study, as total AKT expression and activity were not impacted by loss of a specific isoform, a compensatory mechanism directly regulating the AKT isoform expressions is likely and further investigations are needed to understand the mechanistic basis of this effect. Inhibition of AKT activity through its phosphorylation and not protein levels led however to a significant decrease in cell proliferation associated with an increase in cell death through a strong decrease in MYCN expression. This result is consistent with a study showing that activation of AKT correlates with poor prognosis in primary neuroblastoma,[24] confirming that targeting AKT activity presents a clinically relevant strategy in neuroblastoma.

For many years, AKT has been considered as an attractive target for cancer therapy and prevention, including for neuroblastoma patients.[12] AKT inhibitors have taken a large step forward through the development of compounds that target total AKT or AKT specific isoforms.[15,16] In this study, we used three different AKT inhibitors: AKT1- and AKT2-specific isoform inhibitors and the pan-AKT inhibitor perifosine. Perifosine has been described as an allosteric catalytic inhibitor, which indirectly inhibits the activation of all isoforms of AKT by preventing their translocation to the membrane.[34] Perifosine is moreover an attractive candidate for neuroblastoma treatment as the drug has successfully completed phase I trial investigation with a good safety and tolerability profile in children.[35] Here, in accord with our functional study, only the allosteric pan-AKT inhibitor perifosine led to a strong and constant inhibition of AKT phosphorylation associated with a decrease in MYCN expression in different neuroblastoma cell lines. A study has demonstrated that several small-molecule PI3K/mTOR inhibitors selectively killed *MYCN*-expressing neuroblastoma cells used as a monotherapy.[36] Our data revealed that therapeutic efficacy of perifosine as a monotherapy is independent of the MYCN status in neuroblastoma, and this is supported by results with two different pan-AKT inhibitors (AKT inhibitor VIII and MK-2206) from the publically available GDSC (Genomics of Drug Sensitivity in Cancer) database. This result may reflect additional mechanisms associated with perifosine efficacy. Previous studies have already demonstrated that perifosine affects other key signal

https://dx.doi.org/10.1021/acsptsci.9b00085
ACS Pharmacol. Transl. Sci. 2020, 3, 148−160

transduction pathways, such as c-Jun *N*-terminal kinase (JNK) and nuclear transcription facto κB (NF-κB).[37,38]

To date, only allosteric pan-AKT inhibitors have been tested in neuroblastoma. While MK-2206 has only been tested in neuroblastoma preclinical models,[39] perifosine has already shown promising efficacy as a monotherapy in both preclinical models and in patients in early phase trials.[40,41] However, it is likely that therapies targeting the AKT pathway will complement existing treatment regimens in neuroblastoma rather than lead to their replacement. Monotherapies are highly unlikely to cure patients, but drug combinations are necessary for the most-efficacious treatment of cancer, as well as to prevent or delay the development of resistance.[42] Some studies already reported the lack of single-agent activity of perifosine in different human cancers.[43−45] Here, we highlighted that subtoxic concentration of the pan-AKT inhibitor perifosine led to a synergistic interaction with different classes of chemotherapy agents (vincristine, etoposide and doxorubicin) currently used in neuroblastoma treatment. It is notable that all AKT inhibitors tested were however able to increase vincristine efficiency. As microtubule-targeted agents are efficient through inhibition of the AKT pathway, this may explain the synergistic effect observed with all AKT inhibitors.[46] Importantly, by using three different models of neuroblastoma cells with modulation of *MYCN* expression, our *in vitro* results revealed the selectivity of perifosine combination therapy in *MYCN*-amplified neuroblastoma cell lines. Our *in vivo* data definitively attest to the relationship between MYCN expression and the efficacy of perifosine combination therapy. While only a trend was observed in nonamplified SK-N-AS tumor-grafted mice, the drug synergism with vincristine revealed *in vitro* resulted in a significant prolonged median survival in *MYCN*-amplified BE(2)-C tumor-grafted mice. Future studies will focus on identifying the best therapeutic schedules for maximizing the AKT inhibitor combination therapy efficacy.

A significant impediment to the success of cancer chemotherapy is the occurrence of multidrug resistance, which, in many cases, is attributable to overexpression of ABC transporters.[47] Previous studies have demonstrated that AKT inhibition can downregulate MRP1 and P-gp expression.[48−50] Here our results showed that perifosine led to a decrease in both MRP1 and P-gp expression *in vitro* and *in vivo*. However, combined with vincristine *in vivo*, the combination therapy only decreased P-gp expression. Using the dual MRP1-P-gp inhibitor reversan, our results showed no additive or synergistic effect with perifosine, suggesting that the efficacy of perifosine combined with vincristine does not rely on MRP1 and P-gp expression. Finally, our results demonstrated that drug combination was well-tolerated and did not result in increased toxicity, suggesting that combining perifosine with current cytotoxic drugs could be a promising strategy to develop less toxic and more efficient treatment for children suffering from *MYCN*-amplified neuroblastoma.

The potential applications of AKT inhibitors are numerous. However, to maximally exploit the clinical potential of AKT inhibitors well-designed trials will be required taking into account tolerable clinical schedules, appropriate combinations, and patient selection biomarkers. Here, our findings advance knowledge on the complexity of AKT functions that are likely cancer type specific and context dependent. Our results provide a strong rationale for the advancement and translation of pan-AKT inhibitors rather than isoform-specific drugs as drug sensitizers for patients with *MYCN*-amplified tumors and potentially other *MYCN*-driven cancer.

MATERIAL AND METHODS

Cell Culture. IMR-32 (RRID: CVCL_0346), SK-N-AS (RRID: CVCL_1700), SK-N-BE(2) (RRID: CVCL_0528), SK−N-FI (RRID: CVCL_1702), SH-EP (RRID: CVCL_0524), and Kelly (RRID: CVCL_2092) were obtained from European Collection of Cell Cultures. SK-N-BE(2)-C (referred as BE(2)-C, RRID: CVCL_0529), LA-N-1 (RRID: CVCL_1827), and SH-SY5Y (RRID: CVCL_0019) were provided by Dr. J. Biedler, Memorial Sloan-Kettering Cancer Center, (New York, NY). SK-N-BE(2)-C is a derivative of SK-N-BE(2) and SH-EP is a derivative of SK-N-SH (RRID: CVCL_0531). Upon receipt, cell master stocks were prepared and cells for experiments were passaged for less than 3 months. Master stock cells were validated by PCR (STR profiling) by Cell Bank Australia or Garvan Institute (Sydney, Australia) within the last 3 years. Human SH-EP/Tet21N cells (RRID: CVCL_9812), derived from SH-EP neuroblastoma cells, express *MYCN* under the control of tetracycline (Tet-off) as previously published,[22] and were kindly provided by Dr. M. Schwab from the German Cancer Research Center (Heidelberg, Germany). SK-N-AS and SH-SY5Y pCDH and pMYCN cells were derived from SK-N-AS and SH-SY5Y cells respectively and were generated in the course of this study by stable transfection with MYCN-expression vector (pCDH-CMV-MCS-EF1-copGFP-T2A-Puro, System Biosciences, CA). Neuroblastoma cell lines were cultured in DMEM or RPMI-1640 media (Life Technologies) supplemented with 10% FBS (ThermoTrace) and 2 mmol/L L-glutamine (Invitrogen). Cells were cultured at 37 °C and 5% CO_2 and regularly screened to ensure the absence of mycoplasma contamination using the MycoAlert MycoPlasma Detection Kit (Lonza, Switzerland).

Drugs and Reagents. Stock solutions of etoposide (Sigma-Aldrich), doxorubicin (Sapphire Bioscience, NSW, Australia), CCT128930 (AKT2 inhibitor, Jomar Life Research, VIC, Australia), MK-2206 (AKT1/2 allosteric inhibitor, Jomar Life Research), and reversan (Chembridge, San Diego, CA) were prepared in dimethyl sulfoxide (DMSO), while vincristine solution (Sigma-Aldrich) and A-674563 (AKT1 inhibitor, Jomar Life Research) was prepared in sterile distilled water. Perifosine (octadecyl-(1,1-dimethyl-piperidinio-4-yl)-phosphate) was purchased from Abcam for *in vitro* studies, and its solution was prepared in sterile distilled water. Stock solutions were kept at −20 °C and were freshly diluted in the culture medium for experiments.

Growth Inhibition Assay. For all cell lines, the number of cells seeded (from 3000 to 7500 cells per well, depending on the cell line) in 96-well plates was first optimized to ensure sustained exponential growth for 4−6 days. For all cell lines, cells were treated 24 h after seeding (with the exception of SK-N-BE(2) and LA-N-1 cells, which were allowed to adhere for 36 h before treatment was initiated) with a range of drug concentrations. After 72 h of drug incubation, metabolic activity was detected by addition of Alamar blue by spectrophotometric analysis. Cell proliferation was determined and expressed as a percentage of untreated control cells. The determination of IC_{50} values was performed using GraphPad Prism software (GraphPad Software Inc., La Jolla, CA).

Drug Combination Study. Cells were treated at 24 or 36 h after seeding with a range of concentrations of chemo-

https://dx.doi.org/10.1021/acsptsci.9b00085
ACS Pharmacol. Transl. Sci. 2020, 3, 148−160

therapeutic drugs alone or chemotherapeutic drugs in combination with AKT inhibitors at the lowest effective concentration (IC_{10}). After 72 h of drug incubation, metabolic activity was detected by addition of Alamar blue followed by spectrophotometric analysis. Cell proliferation was determined and expressed as a percentage of untreated control cells. The determination of IC_{50} values was performed using GraphPad Prism software (GraphPad Software Inc., La Jolla, CA). The change in IC_{50} values was calculated by dividing the IC_{50} when chemotherapy agents are used in combination with subtoxic concentrations of AKT inhibitors (IC_{10}) with the IC_{50} when chemotherapy agents are used alone. The combination index (CI) values were calculated with the Calcusyn software according to the Chou and Talalay theorem, which sets out the additive effects (CI = 1), synergisms (CI < 1), and antagonisms (CI > 1) in drug combination.

Spheroid Assay. Cells were seeded in 96-well round-bottomed plates for 48 h. Spheroids were then treated three times per week over 15 days. Images were captured daily with an Olympus microscope (10× /N.A. 0.45 objective lens). Spheroid growth (arbitrary unit, AU) was calculated by measuring the spheroid area with ImageJ software. Spheroid cell survival was measured by adding 10 μL of Alamar Blue per well during 24 h. Absorbance was measured by spectrophotometry Victor plate reader (PerkinElmer, Melbourne, VIC, Australia). Results were expressed as a percentage of spheroid survival compared with no treatment condition. Data displayed are the mean ± SEM of the combined data from three independent biological replicates.

Trypan Blue Dye Exclusion Assay. Cells were cultured in 6-well plates, and cell number and viability were quantified by Trypan Blue staining and cell counting at indicated time points. Data displayed are the mean ± SEM of the combined data from three independent biological replicates.

Colony Forming Assay. Cells were seeded for 6 h prior to the addition of various drugs as indicated in the figure legends. After 72 h of incubation, the drug-containing medium was removed and replaced with complete growth medium. Colonies were simultaneously fixed and stained with 0.5% crystal violet in methanol after 7−10 days depending on the cell line. Individual stained colonies in each well were counted using ImageJ software. Data displayed are the mean ± SEM of the combined data from three independent biological replicates.

Transfection Study. siRNAs used were AKT1 no. 1 (Flexitube siRNA Hs AKT1_5 SI0299149, Qiagen), AKT1 no. 2 (Flexitube siRNA Hs AKT1_7 SI0299159, Qiagen), AKT2 no. 1 (Flexitube siRNA Hs AKT2_6 SI0299173, Qiagen), and AKT2 no. 2 (Flexitube siRNA Hs AKT2_5 SI0299173, Qiagen). siRNA control (Allstars neg Control siRNA 1027781, Qiagen) was used as control for effects of the transfected siRNA at 20 or 50 nM depending on the cell lines. Cells were transfected using Lipofectamine 2000 or RNAiMax (Invitrogen) according to the protocol supplied by the manufacturer. On occasions of double siRNA, total nucleic acid was equalized to the total amount transfected in comparative control samples. After transfection, cells were harvested at 24 h after transfection. Cells were seeded on 96-well round-bottomed plates for cell spheroid assay (Alamar Blue Assay), 6-well plates for colony assay, proliferation assay (Trypan Blue dye exclusion assay), and protein lysate. Data displayed are the mean ± SEM of the combined data from three independent biological replicates.

Western Blot Analysis. Cells were lysed at the time indicated in RIPA buffer (Tris-HCl 50 mM pH 8.0, NaCl 250 mM, Triton-X100 0.1%) with a freshly added cocktail of proteases and phosphatase inhibitors (Sigma-Aldrich). Protein concentrations were determined using the BCA assay kit reagents (Pierce). Proteins were separated by SDS-PAGE and electrotransferred onto a nitrocellulose membrane. The primary antibodies used were directed against GAPDH (1/20 000; no. ab8245; Abcam), pAKT-S473 (1/2000; D9E; no. 4060; Cell Signaling), AKT1 (1/5000; 2H10; no. 2967; Cell Signaling), AKT2 (1/2000; D6G4; no. 3063; Cell Signaling), AKT3 (1/1000; 62A8; no. 3788; Cell Signaling), AKT-total (1/5000; 11E7; no. 4685; Cell Signaling), pGSK3β-S9 (1/2000; D2Y9Y; no. 14630; Cell Signaling), GSK3β-total (1/5000; 3D10: no. 9832; Cell Signaling), PARP (1/2000; no. 9542; Cell Signaling) and MYCN (1/1000; B8.4.B; no. sc53993; Santacruz), MRP1 (1/500; no. ALX-801-007-C125; Sapphire Bioscience), P-gp antibody (1/200; no. NB600−1036; Novus Biologicals) and Na^+/K^+ ATPase (1/1000; no. sc-28800; Santa Cruz). Peroxydase-conjugated secondary antibodies and ECL Plus Western Blotting Detection Reagent (Thermo Fisher Scientific, Victoria, Australia) were used for visualization using ChemiDoc Touch Imaging System (BioRad), and signal quantification was done with ImageJ software. Ratios were calculated as follows: AKT isoforms and phosphorylation normalized to total AKT, pGSK3β-S9 were normalized to total GSK3β and MYCN, total AKT and total GSK3β were normalized to GAPDH.

***In Vivo* Animal Model.** Animal studies were approved by the Animal Ethics Committee at UNSW Australia (AEC no. 17−133B). Female BALB/c nude mice (6−8 weeks old) were obtained from the Australian Bio Resources Facility (Moss Vale, New South Wales, Australia). Cells (1×10^6 BE(2)-C or 0.5×10^6 SK-N-AS) were suspended in 50 μL PBS/50 μL matrigel (Corning, NY) and were inoculated subcutaneously into the flanks of the nude mice. Experimental treatments were started when tumor reached about 100 mm^3 in volume (day 0). Initial pilot studies (n = 4/group) were realized to access the dose response of perifosine and vincristine as single agents. Vincristine was dissolved in injectable saline and administered by consecutive daily i.v. injections for 5 days at three different concentrations: 0.05, 0.1, and 0.2 mg/kg after anesthesia with 3% gaseous isoflurane as previously described in the literature. Perifosine (Jomar Life Research) was dissolved in sterile PBS and was given by oral gavage 5 days/week at 10, 15, or 20 mg/kg as previously described in the literature. The weight of mice was daily determined. Twice a week, tumor volumes were determined by caliper measurements, according to the formula length × width × depth ×0.5236. Mice were sacrificed when their tumor volume exceeded 1000 mm^3. For the survival study, mice (n = 8/group) were allowed to live until their natural death or were sacrificed when their tumor volume exceeded 1000 mm^3 or their weight decrease in more than 20%. Survival medians were estimated by the Kaplan−Meier product limit method. The log-rank test was used to compare survival rates by univariate analysis. One mouse was excluded of the study due to an absence of engraftment. A short-term *in vivo* study was realized for the *MYCN*-amplified BE(2)-C xenografts. Mice (n = 4/group) were humanely killed at 1 week post-treatment, and tumor tissue was excised, measured, and collected for biochemical analysis.

Statistical Analysis. Each experiment was performed at least in triplicate. Data are presented as mean ± SEM.

https://dx.doi.org/10.1021/acsptsci.9b00085
ACS Pharmacol. Transl. Sci. 2020, 3, 148−160

Statistical significance was tested using unpaired Student's *t*-test. For experiments using multiple variables, statistical significance was assessed *via* two-way ANOVA. A significant difference between two conditions was recorded: *, $p < 0.05$; **, $p < 0.01$; ***, $p < 0.001$.

■ ASSOCIATED CONTENT

Supporting Information

The Supporting Information is available free of charge at https://pubs.acs.org/doi/10.1021/acsptsci.9b00085.

Western blot analysis of AKT3 and MYCN in protein extracts from a panel of neuroblastoma cell lines, additional experimental details in different neuroblastoma cell lines or different AKT inhibitors, supporting information of the role of MRP1 and P-gp in drug response in neuroblastoma, additional in vivo experimental details (PDF)

■ AUTHOR INFORMATION

Corresponding Author

Maria Kavallaris − *Children's Cancer Institute, Lowy Cancer Research Centre, UNSW, Sydney 2052, Australia; ARC Centre of Excellence in Convergent Bio-Nano Science and Technology, Australian Centre for Nanomedicine and School of Women's and Children's Health, Faculty of Medicine, UNSW, Sydney 2052, Australia*; Phone: +61-2-9385-2151; Email: m.kavallaris@ccia.unsw.edu.au; Fax: +61-2-9662-6583

Authors

Marion Le Grand − *Children's Cancer Institute, Lowy Cancer Research Centre, UNSW, Sydney 2052, Australia; ARC Centre of Excellence in Convergent Bio-Nano Science and Technology, Australian Centre for Nanomedicine and School of Women's and Children's Health, Faculty of Medicine, UNSW, Sydney 2052, Australia;* orcid.org/0000-0002-4910-1289

Kathleen Kimpton − *Children's Cancer Institute, Lowy Cancer Research Centre, UNSW, Sydney 2052, Australia; ARC Centre of Excellence in Convergent Bio-Nano Science and Technology, Australian Centre for Nanomedicine, UNSW, Sydney 2052, Australia*

Christine C. Gana − *Children's Cancer Institute, Lowy Cancer Research Centre, UNSW, Sydney 2052, Australia; School of Women's and Children's Health, Faculty of Medicine, UNSW, Sydney 2052, Australia*

Emanuele Valli − *Children's Cancer Institute, Lowy Cancer Research Centre, UNSW, Sydney 2052, Australia; School of Women's and Children's Health, Faculty of Medicine, UNSW, Sydney 2052, Australia*

Jamie I. Fletcher − *Children's Cancer Institute, Lowy Cancer Research Centre, UNSW, Sydney 2052, Australia; School of Women's and Children's Health, Faculty of Medicine, UNSW, Sydney 2052, Australia;* orcid.org/0000-0003-2949-9469

Complete contact information is available at: https://pubs.acs.org/10.1021/acsptsci.9b00085

Author Contributions

M.L.G. wrote the manuscript, performed the experiments, and interpreted the data. K.K. performed the *in vivo* study. E.V. and C.C.G. participated in performing experiments and analysis of data. J.I.F. participated in analysis of data and preparation of the manuscript. M.K. supervised the entire study and participated in interpretation of data and preparation of the manuscript. All authors read and approved the final manuscript.

Notes

The authors declare no competing financial interest.

■ ACKNOWLEDGMENTS

This work was supported by the Children's Cancer Institute, which is affiliated with the University of New South Wales (UNSW Australia), and the Sydney Children's Hospital Network; M.K. was supported by grants from The Kids Cancer Project, National Health and Medical Research (Program Grant APP1091261 and Principal Research Fellowship APP1119152). M.K. is also supported by Australian Research Council Centre of Excellence in Convergent Bio-Nano Science and Technology (CE140100036). M.L.G. was supported by an "Unicancer − Fondation de France" fellowship. C.C.G. was supported by Australian Government Research Training Program Scholarship.

■ ABBREVIATIONS

FC: fold-change; siRNA: small interference RNA

■ REFERENCES

(1) Maris, J. M. (2010) Recent advances in neuroblastoma. *N. Engl. J. Med. 362*, 2202−2211.

(2) Irwin, M. S., and Park, J. R. (2015) Neuroblastoma: paradigm for precision medicine. *Pediatr. Clin. North Am. 62*, 225−256.

(3) Matthay, K. K., Maris, J. M., Schleiermacher, G., Nakagawara, A., Mackall, C. L., Diller, L., and Weiss, W. A. (2016) Neuroblastoma. *Nat. Rev. Dis Primers 2*, 16078.

(4) Dang, C. V. (2012) MYC on the path to cancer. *Cell 149*, 22−35.

(5) Brodeur, G. M., Seeger, R. C., Schwab, M., Varmus, H. E., and Bishop, J. M. (1984) Amplification of N-myc in untreated human neuroblastomas correlates with advanced disease stage. *Science 224*, 1121−1124.

(6) Seeger, R. C., Brodeur, G. M., Sather, H., Dalton, A., Siegel, S. E., Wong, K. Y., and Hammond, D. (1985) Association of multiple copies of the N-myc oncogene with rapid progression of neuroblastomas. *N. Engl. J. Med. 313*, 1111−1116.

(7) Weiss, W. A., Aldape, K., Mohapatra, G., Feuerstein, B. G., and Bishop, J. M. (1997) Targeted expression of MYCN causes neuroblastoma in transgenic mice. *EMBO J. 16*, 2985−2995.

(8) Barone, G., Anderson, J., Pearson, A. D., Petrie, K., and Chesler, L. (2013) New strategies in neuroblastoma: Therapeutic targeting of MYCN and ALK. *Clin. Cancer Res. 19*, 5814−5821.

(9) Huang, M., and Weiss, W. A. (2013) Neuroblastoma and MYCN. *Cold Spring Harbor Perspect. Med. 3*, a014415.

(10) Bellacosa, A., Kumar, C. C., Di Cristofano, A., and Testa, J. R. (2005) Activation of AKT kinases in cancer: implications for therapeutic targeting. *Adv. Cancer Res. 94*, 29−86.

(11) Romano, G. (2013) The role of the dysfunctional akt-related pathway in cancer: establishment and maintenance of a malignant cell phenotype, resistance to therapy, and future strategies for drug development. *Scientifica 2013*, 317186.

(12) King, D., Yeomanson, D., and Bryant, H. E. (2015) PI3King the lock: targeting the PI3K/Akt/mTOR pathway as a novel therapeutic strategy in neuroblastoma. *J. Pediatr. Hematol./Oncol. 37*, 245−251.

(13) Chesler, L., Schlieve, C., Goldenberg, D. D., Kenney, A., Kim, G., McMillan, A., Matthay, K. K., Rowitch, D., and Weiss, W. A. (2006) Inhibition of phosphatidylinositol 3-kinase destabilizes Mycn protein and blocks malignant progression in neuroblastoma. *Cancer Res. 66*, 8139−8146.

(14) Chanthery, Y. H., Gustafson, W. C., Itsara, M., Persson, A., Hackett, C. S., Grimmer, M., Charron, E., Yakovenko, S., Kim, G.,

Matthay, K. K., and Weiss, W. A. (2012) Paracrine signaling through MYCN enhances tumor-vascular interactions in neuroblastoma. *Sci. Transl. Med. 4*, 115ra3.
(15) Brown, J. S., and Banerji, U. (2017) Maximising the potential of AKT inhibitors as anti-cancer treatments. *Pharmacol. Ther. 172*, 101−115.
(16) Janku, F., Yap, T. A., and Meric-Bernstam, F. (2018) Targeting the PI3K pathway in cancer: are we making headway? *Nat. Rev. Clin. Oncol. 15*, 273−291.
(17) Manning, B. D., and Toker, A. (2017) AKT/PKB Signaling: Navigating the Network. *Cell 169*, 381−405.
(18) Dillon, R. L., Marcotte, R., Hennessy, B. T., Woodgett, J. R., Mills, G. B., and Muller, W. J. (2009) Akt1 and akt2 play distinct roles in the initiation and metastatic phases of mammary tumor progression. *Cancer Res. 69*, 5057−5064.
(19) Chin, Y. R., Yuan, X., Balk, S. P., and Toker, A. (2014) PTEN-deficient tumors depend on AKT2 for maintenance and survival. *Cancer Discovery 4*, 942−955.
(20) Franks, S. E., Briah, R., Jones, R. A., and Moorehead, R. A. (2016) Unique roles of Akt1 and Akt2 in IGF-IR mediated lung tumorigenesis. *Oncotarget 7*, 3297−3316.
(21) Nicos, M., Krawczyk, P., Jarosz, B., Sawicki, M., Trojanowski, T., and Milanowski, J. (2017) Prevalence of NRAS, PTEN and AKT1 gene mutations in the central nervous system metastases of non-small cell lung cancer. *Brain Tumor Pathol. 34*, 36−41.
(22) Rudolph, M., Anzeneder, T., Schulz, A., Beckmann, G., Byrne, A. T., Jeffers, M., Pena, C., Politz, O., Kochert, K., Vonk, R., and Reischl, J. (2016) AKT1 (E17K) mutation profiling in breast cancer: prevalence, concurrent oncogenic alterations, and blood-based detection. *BMC Cancer 16*, 622.
(23) Dutt, A., Salvesen, H. B., Greulich, H., Sellers, W. R., Beroukhim, R., and Meyerson, M. (2009) Somatic mutations are present in all members of the AKT family in endometrial carcinoma. *Br. J. Cancer 101*, 1218−1219. Author reply: Shoji, K., Oda, K., Nakagawa, S., Hosokawa, S., Nagae, G., Uehara, Y., Sone, K., Miyamoto, Y., Hiraike, H., Hiraike-Wada, O., et al. (2009) Reply: Somatic mutations are present in all members of the AKT family in endometrial carcinoma. *Br. J. Cancer 101*, 1220−1221.
(24) Opel, D., Poremba, C., Simon, T., Debatin, K. M., and Fulda, S. (2007) Activation of Akt predicts poor outcome in neuroblastoma. *Cancer Res. 67*, 735−745.
(25) Robey, R. W., Pluchino, K. M., Hall, M. D., Fojo, A. T., Bates, S. E., and Gottesman, M. M. (2018) Revisiting the role of ABC transporters in multidrug-resistant cancer. *Nat. Rev. Cancer 18*, 452−464.
(26) Fruci, D., C. S. Cho, W., Romania, P., Nobili, V., Locatelli, F., and Alisi, A. (2016) Drug Transporters and Multiple Drug Resistance in Pediatric Solid Tumors. *Curr. Drug Metab. 17*, 308−316.
(27) Burkhart, C. A., Watt, F., Murray, J., Pajic, M., Prokvolit, A., Xue, C., Flemming, C., Smith, J., Purmal, A., Isachenko, N., Komarov, P. G., Gurova, K. V., Sartorelli, A. C., Marshall, G. M., Norris, M. D., Gudkov, A. V., and Haber, M. (2009) Small-molecule multidrug resistance-associated protein 1 inhibitor reversan increases the therapeutic index of chemotherapy in mouse models of neuroblastoma. *Cancer Res. 69*, 6573−6580.
(28) Stottrup, C., Tsang, T., and Chin, Y. R. (2016) Upregulation of AKT3 Confers Resistance to the AKT Inhibitor MK2206 in Breast Cancer. *Mol. Cancer Ther. 15*, 1964−1974.
(29) Virtakoivu, R., Pellinen, T., Rantala, J. K., Perala, M., and Ivaska, J. (2012) Distinct roles of AKT isoforms in regulating beta1-integrin activity, migration, and invasion in prostate cancer. *Mol. Biol. Cell 23*, 3357−3369.
(30) Dummler, B., and Hemmings, B. A. (2007) Physiological roles of PKB/Akt in development and disease. *Biochem. Soc. Trans. 35*, 231−235.
(31) Zitzmann, K., Vlotides, G., Brand, S., Lahm, H., Spöttl, G., Göke, B., and Auernhammer, C. J. (2012) Perifosine-mediated Akt inhibition in neuroendocrine cells: role of specific Akt isoforms. *Endocr.-Relat. Cancer 19* (3), 423−43.
(32) Linnerth-Petrik, N. M., Santry, L. A., Petrik, J. J., and Wootton, S. K. (2014) Opposing functions of Akt isoforms in lung tumor initiation and progression. *PLoS One 9* (4), No. e94595.
(33) Sanchez-Gurmaches, J., Martinez-Calejman, C., Jung, S. M., Li, H., and Guertin, D. A. (2019) Brown fat organogenesis and maintenance requires AKT1 and AKT2. *Mol. Metab. 23*, 60−74.
(34) Mundi, P. S., Sachdev, J., McCourt, C., and Kalinsky, K. (2016) AKT in cancer: new molecular insights and advances in drug development. *Br. J. Clin. Pharmacol. 82*, 943−956.
(35) Kushner, B. H., Cheung, N. V., Modak, S., Becher, O. J., Basu, E. M., Roberts, S. S., Kramer, K., and Dunkel, I. J. (2017) A phase I/Ib trial targeting the Pi3k/Akt pathway using perifosine: Long-term progression-free survival of patients with resistant neuroblastoma. *Int. J. Cancer 140*, 480−484.
(36) Vaughan, L., Clarke, P. A., Barker, K., Chanthery, Y., Gustafson, C. W., Tucker, E., Renshaw, J., Raynaud, F., Li, X., Burke, R., Jamin, Y., Robinson, S. P., Pearson, A., Maira, M., Weiss, W. A., Workman, P., and Chesler, L. (2016) Inhibition of mTOR-kinase destabilizes MYCN and is a potential therapy for MYCN-dependent tumors. *Oncotarget 7*, 57525−57544.
(37) Fu, L., Lin, Y. D., Elrod, H. A., Yue, P., Oh, Y., Li, B., Tao, H., Chen, G. Z., Shin, D. M., Khuri, F. R., and Sun, S. Y. (2010) c-Jun NH2-terminal kinase-dependent upregulation of DR5 mediates cooperative induction of apoptosis by perifosine and TRAIL. *Mol. Cancer 9*, 315.
(38) Chen, M. B., Wu, X. Y., Tao, G. Q., Liu, C. Y., Chen, J., Wang, L. Q., and Lu, P. H. (2012) Perifosine sensitizes curcumin-induced anti-colorectal cancer effects by targeting multiple signaling pathways both in vivo and in vitro. *Int. J. Cancer 131*, 2487−2498.
(39) Li, Z., Yan, S., Attayan, N., Ramalingam, S., and Thiele, C. J. (2012) Combination of an allosteric Akt Inhibitor MK-2206 with etoposide or rapamycin enhances the antitumor growth effect in neuroblastoma. *Clin. Cancer Res. 18*, 3603−3615.
(40) Li, Z., Tan, F., Liewehr, D. J., Steinberg, S. M., and Thiele, C. J. (2010) In vitro and in vivo inhibition of neuroblastoma tumor cell growth by AKT inhibitor perifosine. *J. Natl. Cancer Inst 102*, 758−770.
(41) Matsumoto, K., Shichino, H., Kawamoto, H., Kosaka, Y., Chin, M., Kato, K., and Mugishima, H. (2017) Phase I Study of Perifosine Monotherapy in Patients With Recurrent or Refractory Neuroblastoma. *Pediatr Blood Cancer 64* (11), No. e26623.
(42) Rubin, E. H., and Gilliland, D. G. (2012) Drug development and clinical trials–the path to an approved cancer drug. *Nat. Rev. Clin. Oncol. 9*, 215−222.
(43) Posadas, E. M., Gulley, J., Arlen, P. M., Trout, A., Parnes, H. L., Wright, J., Lee, M. J., Chung, E. J., Trepel, J. B., Sparreboom, A., Chen, C., Jones, E., Steinberg, S. M., Daniels, A., Figg, W. D., II, and Dahut, W. L. (2005) A phase II study of perifosine in androgen independent prostate cancer. *Cancer Biol. Ther. 4*, 1133−1137.
(44) Argiris, A., Cohen, E., Karrison, T., Esparaz, B., Mauer, A., Ansari, R., Wong, S., Lu, Y., Pins, M., Dancey, J., and Vokes, E. (2006) A phase II trial of perifosine, an oral alkylphospholipid, in recurrent or metastatic head and neck cancer. *Cancer Biol. Ther. 5*, 766−770.
(45) Knowling, M., Blackstein, M., Tozer, R., Bramwell, V., Dancey, J., Dore, N., Matthews, S., and Eisenhauer, E. (2006) A phase II study of perifosine (D-21226) in patients with previously untreated metastatic or locally advanced soft tissue sarcoma: A National Cancer Institute of Canada Clinical Trials Group trial. *Invest. New Drugs 24*, 435−439.
(46) Le Grand, M., Rovini, A., Bourgarel-Rey, V., Honore, S., Bastonero, S., Braguer, D., and Carre, M. (2014) ROS-mediated EB1 phosphorylation through Akt/GSK3beta pathway: implication in cancer cell response to microtubule-targeting agents. *Oncotarget 5*, 3408−3423.
(47) Gottesman, M. M. (2002) Mechanisms of cancer drug resistance. *Annu. Rev. Med. 53*, 615−627.
(48) Chiarini, F., Del Sole, M., Mongiorgi, S., Gaboardi, G. C., Cappellini, A., Mantovani, I., Follo, M. Y., McCubrey, J. A., and Martelli, A. M. (2008) The novel Akt inhibitor, perifosine, induces

https://dx.doi.org/10.1021/acsptsci.9b00085
ACS Pharmacol. Transl. Sci. 2020, 3, 148−160

caspase-dependent apoptosis and downregulates P-glycoprotein expression in multidrug-resistant human T-acute leukemia cells by a JNK-dependent mechanism. *Leukemia 22*, 1106−1116.

(49) Moon, J. Y., Manh Hung, L. V., Unno, T., and Cho, S. K. (2018) Nobiletin enhances chemosensitivity to adriamycn through modulation of the Akt/GSK3/-catenin/MYCN/MRP1 signaling pathway in A549 human non-small-cell-lung cancer cells. *Nutrients 10* (12), 1829.

(50) Lin, X., Zhang, X., Wang, Q., Li, J., Zhang, P., Zhao, M., and Li, X. (2012) Perifosine downregulates MDR1 gene expression and reverses multidrug-resistant phenotype by inhibiting PI3K/Akt/NF-kappaB signaling pathway in a human breast cancer cell line. *Neoplasma 59*, 248−256.

https://dx.doi.org/10.1021/acsptsci.9b00085
ACS Pharmacol. Transl. Sci. 2020, 3, 148−160